Oct 26th, 12:00 AM

Local and Distortional Buckling of Cold-formed Steel Studs Using Direct Strength

Jennifer Tovar

Eighteenth International Specialty Conference on Cold-Formed Steel Structures
Orlando, Florida, U.S.A, October 26 & 27, 2006

Local and Distortional Buckling of Cold-Formed Steel Studs Using Direct Strength

Jennifer Tovar[1] and Thomas Sputo[2]

Abstract

A study to develop methods of analyzing perforated, axially loaded, cold-formed steel studs using the provisions of the Direct Strength Method was undertaken using the Finite Strip Method as the method for determining the elastic buckling stresses. Several different models were developed to represent the effect of typical C-section web perforations. Distortional buckling strength predictions obtained in this study never controlled the overall buckling capacity of a stud. The capacities predicted using the Direct Strength Method for the limit states of distortional and local buckling were compared to capacities calculated using the effective width equations contained in the AISI *Specification*. The validity of the results is discussed and recommendations are made for the use of the Direct Strength Method for these members.

Introduction

This is the second of two companion papers in which the use of the direct strength method for design of perforated cold-formed steel studs in axial compression is studied. The first paper (Sputo and Tovar, 2006), considered the limit state of longwave buckling, while this paper considers the limit states of distortional and local buckling. For further background information on the Direct Strength Method, the Finite Strip Method of analysis, and the development of cross section models, refer to Tovar and Sputo (2005).

[1] Graduate Student, Dept. of Civil, Architectural & Environmental Engrg., Univ. of Texas, Austin, TX 78712-0273; Formerly Undergraduate Student, Dept. of Civil & Coastal Engrg., 365 Weil Hall, Univ. of Florida, Gainesville, FL 32611 (email: jennifer@ schwabse.com).
[2] Senior Lecturer, Dept. of Civil & Coastal Engrg., 365 Weil Hall, University of Florida, Gainesville, FL 32611; Structural Engineer, Sputo and Lammert Engrg., LLC, 10 SW 1st Ave., Gainesville FL 32601. (email: sputo@ufl.edu)

Distortional Buckling

Distortional buckling involves both rotation and translation at the corners of the cross-section. This is observed as a distortion of the cross section when one portion of the section is "forced out" by a more rigid response of the remaining portion (Figure 1). In some cases this mode may be somewhat indistinct, however stiffened flanges make it particularly easy to distinguish between distortional and local buckling for C sections.

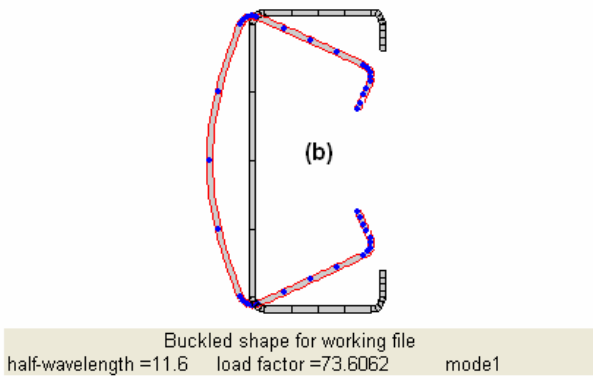

Figure 1. Distortional Buckling from CUFSM Output for 362S162-68 (Figure units in English system)

Distortional buckling will typically occur in the second "dip" of the buckling curve (Point B, Figure 2). This will usually appear over half-wavelengths that are two to four times the section web height. Ideally, a local minimum will occur in this range making it easy to determine the controlling critical buckling stress for distortional buckling. Where no local minimum was apparent, which was often the case in this study, higher order modes were used to 'extrapolate' the critical buckling stress. Further explanation of such determinations is discussed in Tovar and Sputo (2005).

The critical elastic load, P_{crd} , for distortional buckling (Schafer, 2002) may be obtained from

$$P_{crd} = F_{crd} * A_g \qquad \text{(Eq. 1)}$$

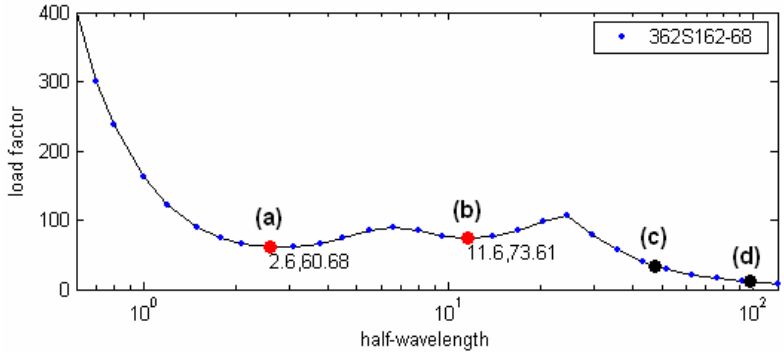

Figure 2. CUFSM Section Model Analysis Output for 362S162-68
(Figure units in English system)

where F_{crd} = Critical buckling stress for distortional buckling

A_g = Area of the section

The nominal axial strength, P_{nd}, for distortional buckling is

for $\lambda_d \le 0.561 \quad P_{nd} = P_y$ (Eq. 2)

for $\lambda_d > 0.561 \quad P_{nd} = \left[1 - 0.25\left(\frac{P_{crd}}{P_y}\right)^{0.6}\right]\left(\frac{P_{crd}}{P_y}\right)^{0.6} P_y$ (Eq. 3)

where $\lambda_d = \sqrt{P_y / P_{crd}}$ (Eq. 4)

P_{crd} = Critical elastic distortional column buckling load according to elastic buckling requirements

Direct Strength Method (DSM) equations were used to calculate nominal axial strength for the distortional buckling mode. Analysis was performed for representative sections (See Table 1 in Sputo and Tovar, 2006) and calculations were performed for unbraced lengths of 1219 and 2438 mm and yields strengths of 227.5 and 344.7 MPa.

Solid Web Model – Distortional Buckling Results

The solid web model is the base model for analysis and is applicable for calculation of the distortional buckling capacity. A description of the solid web model, along with an illustration, is found in a companion paper by Sputo and Tovar (2006). The main body of the AISI *Specification* does not account for distortional buckling, therefore no direct comparison of these results can be made to the AISI *Specification*. Furthermore, it was found that distortional bucking was never the controlling limit state for the studs analyzed in this study. As a result, distortional buckling is evaluated and discussed more for its interactions in the local and longwave buckling results.

Distortional interaction in CUFSM local buckling predictions was occasionally evident for sections with a flatter buckling curve. This influence was generally of very little significance and was accounted for as described in the local buckling section. A more detailed record of the distortional influence in local buckling results is contained in Tovar and Sputo (2005).

There was a notable interaction from distortional buckling in some of the long-wave buckling results. The role of distortional interaction in longwave buckling results is covered in more detail in the companion paper (Sputo & Tovar, 2006).

Equivalent-Thickness Model – Distortional Buckling Results

The equivalent-thickness model (Sputo and Tovar, 2006) was developed to distribute the effects of the holes along the length of the stud. Distortional buckling half-wavelengths do not encompass as much material along the entire length of the stud, hence the averaging effect of the equivalent thickness method is most likely not as applicable for distortional buckling. Consequently, equivalent-thickness model results have not been included for this limit state.

Perforated Web Model – Distortional Buckling Results

The perforated web model (Sputo and Tovar, 2006) is used to predict strength at locations of the punchout. This model is most appropriate for buckling modes whose half-wavelength is less than the length of the perforation. Distortional buckling however, occurs at a half-wavelength at least two to three times greater than the perforation length. For this reason, the perforated model is assumed not applicable for the limit state of distortional buckling. Additional research in this area, including Finite Element Analysis studies, is necessary to produce a complete understanding of the interaction of distortional buckling with web perforations.

Local Buckling

Local buckling occurs in one or more cross-sectional elements (web or flanges) but does not involve any displacement or translation of the corner nodes (Figure 3). For most C-sections, the critical buckling stress for local buckling will occur at an apparent minimum in the first "dip" of the buckling curve (Point A, Figure 2). This minimum will be at a half-wavelength less than the overall height of

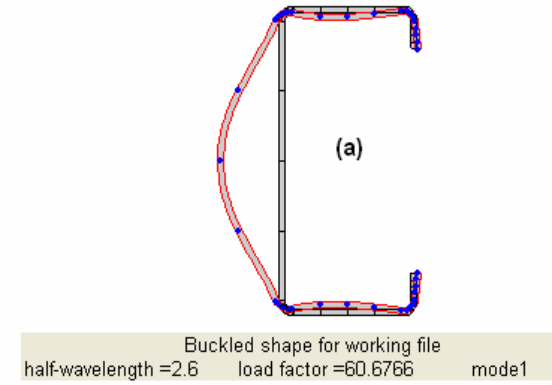

Figure 3. Local Buckling from CUFSM Output for 362S162-68 (Figure units in English system)

the web. For most sections analyzed, CUFSM marked the appropriate minimum value on the curve. Only a few very stocky sections (low web/thickness ratios with wide flanges) had minimums which occurred outside these local definitions and a critical stress was taken at a value slightly higher than the marked minimum where a "purer" locally buckled shape was observed. Representative sections (Sputo and Tovar, 2006) were analyzed and calculations were performed for unbraced lengths of 1219 and 2438 mm and yield strengths of 227.5 and 344.7 MPa using the following equations.

The critical elastic load, P_{crl}, for local buckling (Schafer, 2002) may be obtained from

$$P_{crl} = F_{crl} * A_g \qquad \text{(Eq. 5)}$$

where F_{crl} = Critical buckling stress for local buckling

A_g = Area of the section

The nominal axial strength, P_{nl}, for local buckling is

for $\lambda_l \le 0.776 \quad P_{nl} = P_{ne}$ (Eq. 6)

for $\lambda_l > 0.776 \quad P_{nl} = \left[1 - 0.15\left(\frac{P_{crl}}{P_{ne}}\right)^{0.4}\right]\left(\frac{P_{crl}}{P_{ne}}\right)^{0.4} P_{ne}$ (Eq. 7)

where:

for $\lambda_c \le 1.5 \quad P_{ne} = \left(.658^{\lambda_c^2}\right)P_y$ (Eq. 8)

for $\lambda_c > 1.5 \quad P_{ne} = \left(\frac{.877}{\lambda_c^2}\right)P_y$ (Eq. 9)

$$\lambda_c = \sqrt{P_y / P_{cre}} \quad \text{(Eq. 10)}$$

$$P_y = A_g F_y \quad \text{(Eq. 11)}$$

P_{cre} = Minimum of the critical elastic column buckling load for flexural, torsional, or torsional-flexural buckling according to the elastic buckling stress

$$\lambda_l = \sqrt{P_y / P_{crl}} \quad \text{(Eq. 12)}$$

P_{crl} = Critical elastic local column buckling load according to elastic buckling requirements

Solid Web Model – Local Buckling Results

The solid web model is the base model for analysis and is applicable to the calculation of local buckling capacity. A description of the solid web model is found in Sputo and Tovar (2006).

DSM predictions where local buckling controlled were compared to AISI *Specification* (2004) results and summarized in Table 1. It can be seen that DSM predictions for the few local buckling controlled 362S162 studs compare favorably with normalized DSM/AISI nominal capacity ratios. However, the DSM strength predictions for the remainder of the studs diverge when compared to the AISI specification predictions. This divergence was previously noted by Schafer (2000) as the result of flaws in the AISI specification effective width procedure which ignores web-flange interaction where high web slenderness drives the stability of the flange. As reported by Schafer, the strength predicted by the DSM matches tested capacities much better than AISI equivalent width predictions.

Table 1. Summarized Solid Web Local Buckling

Stud SERIES	DSM/AISI	
	MEAN	ST DEV
362S162	1.040	0.084
600S162	0.967	0.082
800S162	0.907	0.171
600S250	0.886	0.098
800S250	0.801	0.164
Total	0.920	0.090

The increased divergence in the DSM local buckling predictions when compared to the AISI effective width method was found to be directly related to the height to thickness (h/t) ratio of the stud web. Figure 4 contains a graphical illustration of this trend. Predictions for the unbraced length of 1219 mm diverge more than the 2438 mm predictions. This difference is accounted for in that longwave buckling has a greater influence at the longer unbraced length. The divergence noted here strengthens the necessity for reevaluation of the AISI effective width method for slender webs in compression.

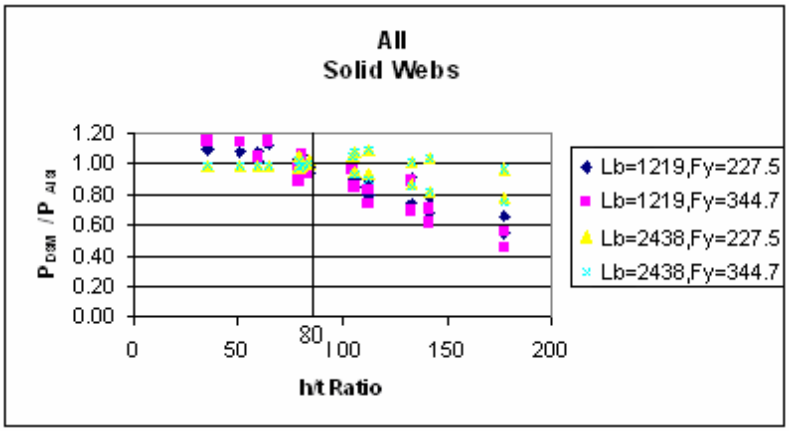

Figure 4. Nominalized DSM/AISI axial capacity vs. h/t ratios for all studs

Equivalent-Thickness Model – Local Buckling Results

The equivalent-thickness model was developed to distribute the effects of the holes along the length of the stud. Each local buckling half-wavelength

encompass only a small fraction of the material along the length of the stud, therefore the averaging effect of the equivalent-thickness method is not considered applicable to local buckling. For this reason, equivalent-thickness model results have not been included in the calculations for this limit state.

Perforated Web Model – Local Buckling Results

The perforated web model was designed to predict critical buckling stress at the location of the perforation. Local buckling half-wavelengths occur at lengths less than the height of the stud web. Therefore one local buckling half-wavelength could occur over the punchout, while the adjacent two to seven half-wavelengths may occur over a solid web (See Figure 2 in Sputo and Tovar, 2006). Consequently, these conditions are examined independently. The perforated model was used to examine local buckling capacity at the punchout location and the solid model was used to examine local bucking capacity at locations away from the punchout. This simplification ignores longitudinal compatibility (buckling wavelength in the web and perforated portions of the plate influencing each other). Further description of the perforated web model is found in Sputo and Tovar (2006). More comprehensive tabular results for this limit state are available in Tovar and Sputo (2005).

Perforated Web Strength Comparison

DSM predictions for the perforated web model resulted in local buckling as the controlling limit for nearly all the same sections as the solid model. Exceptions for which perforated model local buckling did not control included the 362S162-43 (227.5 MPa only), 362S162-68 (344.7 MPa only), and 800S162-68 studs for 1419 mm unbraced lengths and 800S162-54 studs for 2438 mm unbraced lengths. The 600S250-97 perforated stud was controlled by local buckling at the 1419 mm unbraced length with a yield stress of 344.7 MPa whereas the equivalent solid stud was not.

DSM Perforated Vs. Solid Strength Comparison

When comparing DSM perforated local buckling capacities to solid local buckling results (Table 2), there was a surprising observation. The local buckling capacities for the perforated model were actually higher than predicted capacities for the solid model for almost all the studs analyzed. The reason for this finding is not readily apparent and requires further study (using FEM).

Table 2. Summarized local buckling strength comparison for DSM perforated and solid web

Stud SERIES	Perforated vs. Solid Comparison DSM_{per}/DSM_{sol}	
	MEAN	ST DEV
362S162	1.150	0.003
600S162	0.984	0.067
800S162	1.039	0.006
600S250	1.027	0.001
800S250	1.052	0.002
Total	1.050	0.061

Comparison of Results

In general, once prequalified studs (both solid and perforated) reach web height to thickness (h/t) ratios greater than 80, DSM predictions for local buckling diverge from the AISI effective width method due to flaws in the AISI effective width method. It is therefore necessary to be aware of this phenomenon when comparing the results of the DSM method to the AISI effective width method. Because the punchout occurs within the ineffective area of the web for sections whose strength is controlled by local buckling, further investigation in this area may validate the observation that perforated buckling results at the punchout are actually higher than solid buckling results away from the punchout. This is not to say that the capacity is higher for a perforated stud than an unperforated stud; it merely speculates that the critical stress required for local buckling to develop over the perforations (where the web briefly transitions from solid and stiffened, to separated and unstiffened, and then back again) may actually be higher than developing in a solid portion of the web. With this confirmation it could be concluded that the solid section gives the most accurate and conservative capacity prediction for both punched and unpunched studs and the perforations can therefore be ignored. Additional Finite Element Analysis studies are clearly needed.

CONCLUSIONS

Distortional Buckling

The distortional buckling strength predictions obtained in this study never controlled for the overall buckling capacity of a stud. However, the interaction of distortional buckling in the critical buckling strengths for local and longwave buckling was apparent in some cases. The critical stresses with the most significant distortional interaction usually did not control, however, this is a phenomenon which should be monitored carefully for cases in which it may become a more controlling factor and results may need to be adjusted accordingly.

Local Buckling

When determining the strength for a punched stud, two models were considered: a solid model for locations away from the punchout and a perforated model for locations at a punchout. The combination of these two models were used to come up with a potentially more accurate strength prediction than the AISI predictions which do not account for any material at the punchout along the full length of the member. In considering the buckling strengths for the separate locations at and away from the punchout, a very surprising and significant trend was observed. The results from this study actually predict higher strengths for the perforated model than the solid model. This seems to indicate that the stud will reach the limit state of local buckling at sections away from the perforation at lower levels of load than at the perforation. Additional study is clearly needed.

Appendix. – References

American Iron and Steel Institute (AISI). (2004). *North American Specification for the Design of Cold-Formed Steel Structural Members 2001 Edition with Supplement 2004 (AISI/COFS/NASPEC 2004) and Commentary (AISI/ COFS/NASPEC 2004)*, Washington, DC.

Schafer, B.W. (2000) "Distortional Buckling of Cold-Formed Steel Columns." Final report to the American Iron and Steel Institute, Washington, DC.

Schafer, B.W. (2002). *Design Manual for Direct Strength Method of Cold-Formed Steel Design, January 2002 Draft.* American Iron and Steel Institute, Washington, DC.

Tovar, J. and Sputo, T. (2005). "Application of direct strength method to axially loaded perforated cold-formed steel studs: Distortional and local buckling." *Thin Walled Structures,* (43) 1882-1912.

Sputo, T. and Tovar, J. (2005). "Application of direct strength method to axially loaded perforated cold-formed steel studs: longwave buckling." *Thin Walled Structures,* (43) 1852-1881.

Sputo, T. and Tovar, J. (2006). "Longwave buckling of cold-formed steel studs using direct strength." *Proceedings of the 18th International Specialty Conference on Cold-Formed Steel Structures*, Orlando, FL.